

Introduction

The Mousterian cave of Barakaevskaia (Barakai) is one of several caves and rockshelters along the Gubs River, located in Borisovskoe Gorge, northern Caucasus (Figure 1). A single Mousterian layer from this cave yielded thousands of flint artifacts, retouched bones, faunal remains and a child's mandible. Based on its robust size, taurodont molars and morphologically complex teeth, Faerman et al (1994) concluded that the mandible belonged to a Neandertal.



Figure 1: Location of Barakai cave

Recent dating of the layer in which the mandible was found places it within the range of 38,950-36,420 cal BP (OxA-23002), roughly contemporaneous with Mezmaiskaya (Skinner et al 2005). This new date, together with the somewhat ambiguous dental morphology (e.g. a divided middle trigonid crest), has prompted us to apply relatively new geometric morphometric techniques to confirm the taxonomic status of the individual. In the process, we examine whether or not the lower deciduous first molar is taxonomically diagnostic. Benazzi et al (2011) have confirmed shape differences (e.g., more ovoid outline) between Neandertals and *H. sapiens* noted in the lower deciduous second molar (Tattersall and Schwartz, 1999; Souday and Bailey, 2011), but the shape of the lower first deciduous molar has not yet been assessed in this way. This study examines variation in the lower deciduous molar shapes of Neandertals, fossil and recent *H. sapiens* and seeks to place the Barakai individual within that context.

Methods

Occlusal images were taken with a Canon Rebel XT and Nikon D80 digital camera or extracted from three-dimensional models based on mCT scans processed at the Max Planck Institute for Evolutionary Anthropology. All teeth were oriented using standard procedures (Bailey 2004). Images were imported into and edited in Adobe Photoshop®. Where the left tooth was not available, the right tooth was photographed and mirror imaged. Backgrounds were removed to ensure maximum contrast and each image was scaled to approximately the same size and resolution (300 dpi).

Outlines were automatically extracted using scripts developed by RI for ImageJ and R (Iovita and McPherron 2011*, Figure 2). Elliptical Fourier analysis (EFA, Kuhl and Giardina, 1982; Ferson et al., 1985) was used to describe the outlines of the dm1 and dm2. Normalized Fourier coefficients were used in order to remove the effects of size, position, and rotation. The elliptic Fourier coefficients for each specimen (from the 2nd to the 8th harmonic) were treated as variables in discriminant function analyses. The d1 coefficient from the first harmonic was retained (the other coefficients, a1-c1 are respectively 1 and 0), as it represents the elongation of the best-fitting ellipse and may contain important shape information. Following Bailey and Lynch (2005), Wilks Lambda was first calculated for MANOVA, then subjected to a permutation test with 10000 iterations. Finally, Barakai was treated as an unknown and reclassified using the LDA, calculating the posterior probabilities of assignment to a particular group.

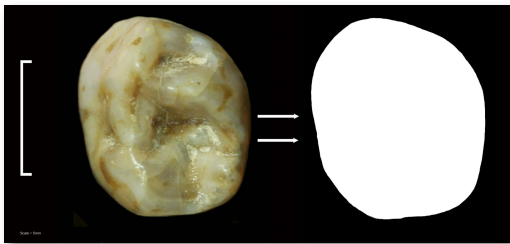


Figure 2: Outline acquisition of lower deciduous first molar

Conclusions

Until very recently the deciduous teeth of Middle-Late Pleistocene hominins were given little attention. This study of the lower dm1 and dm2 provides further evidence of shape differences in the postcanine teeth of Neandertals and *H. sapiens* and demonstrates the utility of deciduous teeth for taxonomic assessment. The Barakai individual is clearly affiliated with Neandertals, confirming its previous taxonomic designation (Faerman et al, 1994). The recent date places it with other late surviving Neandertals in the Caucasus. We are currently investigating meristic variation and the affect of allometry on the shapes of lower dm1, dm2 and M1 (Bailey et al in prep).

Acknowledgements

This research was funded in part by the Science Foundation of Ireland, and the LSB Leakey Foundation. We thank Jean-Jacques Hublin for providing access to 3D reconstructions of certain fossil teeth from the MPI collection, as well as Heiko Temming and Matt Skinner who made and processed any 3D scans used in this analysis.

References

Bailey SE 2004. A morphometric analysis of maxillary molar crowns of Middle-late Pleistocene hominins. *J Hum Evol.* 47: 183-198. • Bailey SE, Lynch JM. 2005. Diagnostic differences in mandibular P4 shape between Neandertals and anatomically modern humans. *Am J Phys Anthropol* 126:268-277 • Benazzi S, Fornai C, Bayle P, Coquerelle M, Kullmer O, Mallegni F, Weber G. 2011. Comparison of dental measurement systems for taxonomic assignment of Neandertal and modern human lower second deciduous molars. *J Hum Evol.* 61(3): 320-326. • Faerman M, Zilberman U, Smith P, Kharitonov V. 1994. A Neandertal infant from the Barakai Cave, Western Caucasus. *J Hum Evol.* 27: 405-15. • Ferson S, Rohlf FJ, Koehn RK. 1985. Measuring shape variation of two-dimensional outlines. *Sys Zool* 34: 59-68. • Iovita R, McPherron SP. 2011. The handaxe reloaded: A morphometric reassessment of Acheulian and Middle Paleolithic handaxes • Kuhl FP, Giardina CR. 1982. Elliptic Fourier Features of a closed contour. *Comput Gr Image Process.* 18: 236-258. • Skinner AR, Blackwell B, Martin S, Ortega A, Bickstein JB, Golovanova LV, Doronichev VB. ESR dating at Mezmaiskaya Cave Russia. *Ap Rad Iso.* 62: 219-224. • Souday C, Bailey SE. 2011. Size and shape analysis of second deciduous molars in the genus *Homo*. *Am J Phys Anthropol* 152: 209 • Tattersall I, Schwartz J. 1999. Hominins and hybrids: the place of Neandertals in human evolution. *PNAS.* 96: 7117-7119.

*also available from <https://radiuovita.wordpress.com/software/>

Materials

Our analysis included the deciduous lower first and second molars of 24 Neandertal, 19 Upper Paleolithic *H. sapiens*, 4 early *H. sapiens*, and 131 recent *H. sapiens* individuals from Africa, Asia, Europe, Australia and the Americas (Table 1).



Table 1

Group	dm1	dm2
<i>H. neanderthalensis</i> (n=24)	n=13	n=18
Archi, Arcy sur Cure, Barakai, Cova Negra, Engis, Krapina, Kebara, La Chaise, La Ferrassie, Fontéchevade, Mezmaiskaya, Molare, Peche de l'Azé, Roc de Marsal, Scladina, Valgadoba		
Upper Paleolithic <i>H. sapiens</i> (n=19)	n=10	n=15
Aveline, Balla Barlang, Combe Capelle, Combe Grenal, Estelas, Figuier, Isturtiz, Kostenki, Lagar Velho, Madeleine, Miesslingtal, Shukbah, Solutre, St. Germain, Sunghir		
Early <i>H. sapiens</i> (n=4)	n=3	n=2
Qafzeh, Die Kelders, Equus Cave		
Recent <i>H. sapiens</i> (n=131)		
Africa (East, South, West, Egypt)	n=62	n=61
India	n=9	n=10
Europe (West, South)	n=38	n=42
South America	n=16	n=16
Australia	n=2	n=2

Results

Figures 3 and 4 plot the individual lower dm1s and dm2s, respectively. For the lower dm1, Neandertals are clearly separated from Upper Paleolithic *H. sapiens* along LD1, showing no overlap between the groups. Adding early *H. sapiens* and recent *H. sapiens* muddies the picture somewhat. EHS are not separated from Neandertals along LD1 but LD2 distinguishes them quite well. Recent *H. sapiens* are somewhat scattered and overlap the Neandertal distribution. They tend to fall in the upper right corner of the plot (positive scores for LD1 and LD2) whereas the Neandertals fall on the lower left corner (negative scores for LD1 and LD2). The outline of the lower dm2 shows a similar pattern, with clear distinction between Upper Paleolithic *H. sapiens* and Neandertals and some recent *H. sapiens* overlapping with the Neandertal distribution. Once again the EHS overlap with Neandertals along LD1 and are better discriminated along LD2.

LD1 accounts for 58.8% of the trace and LD for 31.6% (dm1) and 75.2% and 16.8% (dm2). These linear discriminants are robust at the 0.05 level according to the permutation tests on Wilks Lambda. The Barakai individual classifies as a Neandertal with a posterior probability of 92% based on ldm1 and 87.5% based on ldm2. Not surprisingly, the Barakai individual lies comfortably within the Neandertal distribution for both dm1 and dm2 shapes in Figures 3 and 4.

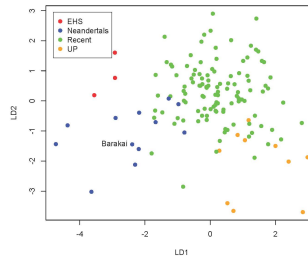


Figure 3: Plot of lower dm1 outlines

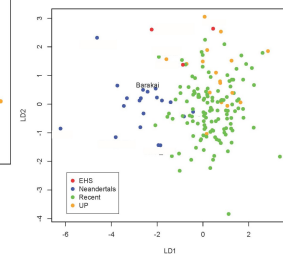


Figure 4: Plot of lower dm2 outlines